High-Quality Photonic Sampling Streams From a Semiconductor Diode Ring Laser

Christopher M. DePriest, Tolga Yilmaz, Alan Braun, Joe Abeles, and Peter J. Delfyett, Jr.

***Abstract*—We report on the development of an ultralow-noise, external-cavity, actively mode-locked semiconductor diode laser for application in next-generation photonic sampling systems. A summary of harmonically mode-locked noise characteristics in a 65-MHz ring cavity is presented through the range of pulse repetition frequencies between 130 MHz and 8.3 GHz (2nd–128th harmonic). Important implications regarding the use of gain-versus-loss modulation as the active modelocking mechanisms are discussed. We also report what are, to our knowledge, the lowest noise characteristics achieved to date for a semiconductor diode laser operating at 10 GHz. Individually optimized results of 0.12% rms amplitude noise (10 Hz–10 MHz), and 43 fs rms residual phase jitter (10 Hz–10 MHz) provide a theoretical resolution of 8.6 bits in a 10-GSPS optical analog-to-digital converter. We have also achieved dispersion-compensated pulsewidths as short as 1.2 ps, and shown successful operation of a novel phase-locked-loop capable of reducing the rms residual phase noise by as much as 91% within its response bandwidth. Finally, the first measurements of residual phase noise out to the Nyquist frequency (5 GHz) are presented, providing an upper bound on the rms residual phase jitter of 121 fs (10 Hz–5 GHz).**

***Index Terms*—Active modelocking, amplitude noise, optical analog-to-digital conversion, phase noise, semiconductor optical amplifiers, timing jitter.**

I. Introduction

THE notion of using optical pulsetrains to sample temporal signals for analog-to-digital conversion has been around for several decades, prompted by the recognition of the considerably greater bandwidth and low wideband dispersion available in the optical domain [1]. Commercially available digital oscilloscopes capable of multigigahertz sampling rates and 8 bits of resolution do exist, but these systems use time-interleaved techniques to achieve high clocking rates, which results in significantly higher amounts of clock jitter. Recently published results using purely electronic, flash-type analog-to-digital converters (ADCs) have shown a capability of 3–6 bits of resolution within the Nyquist band at 8–10 GHz sampling rates [2]–[4]. The desire to increase both bit resolution and sampling rates has inspired the active investigation of a variety of optical approaches [5]–[16]. While many of these strategies show promise, the primary limitations on the accuracy of any high-speed sampling scheme will be determined by noise characteristics [17].

As a foundation for highly accurate clocking and sampling in a next-generation optical ADC, we propose an actively mode-locked external-cavity semiconductor diode ring laser, capable of producing ultralow-noise pulsetrains with repetition rates as high as 20 GHz and pulsewidths as short as 1.2 ps. The purpose of this paper is to present an examination of a broad range of noise effects (as well as techniques for their measurement and control) in one laser system. The wide range of experimental results regarding the noise properties of mode-locked laser systems having greatly varying operating conditions makes it difficult for researchers to perform a fair comparison. This work is intended to provide researchers with a framework by which to assess and compare the noise characteristics of mode-locked diode lasers over a broad range of operating conditions, e.g., repetition rate, oscillator noise, etc.

The paper is organized as follows. The experimental architecture will be discussed in Section II. This is followed in Section III by a comparative survey of laser noise characteristics as a function of both modelocking frequency (cavity harmonic number) and modelocking technique (gain-versus-loss modulation). Noise and pulsewidth characteristics during highly optimized operation at 10 GHz are presented in Section IV, along with a proof-of-principle demonstration (at 2 GHz) of residual phase noise reduction through the use of a novel phase-locked loop. Finally, the implications of extended noise sideband measurements out to Nyquist offset frequencies (5 GHz) are discussed in Section V.

II. Experimental Geometry

A schematic diagram of the laser and peripherals is shown in Fig. 1 [18]. The oscillator ring cavity (longitudinal mode spacing $\sim$65 MHz) consists of a 2.3-mm InGaAsP semiconductor optical amplifier (SOA) and a fiber-pigtailed Mach–Zehnder intensity modulator. The ring is made to be unidirectional by the insertion of two intracavity Faraday isolators. An etalon (FSR $\sim$7 nm, finesse $\sim$5) is inserted in the cavity to limit the mode-locked bandwidth and achieve lowest noise operation. Although broadband multiwavelength pulsetrains have previously been demonstrated using these laser systems [19], [20], the present geometry is implemented in a narrowband, single-wavelength form in order to eliminate the possibility of additional noise due to interwavelength modegroup competition [21]. The etalon is later removed to allow the mode-locked spectrum to broaden for shortest-pulse operation, resulting in slightly higher levels of rms noise. Following the oscillator, a

Manuscript received July 18, 2001; revised December 21, 2001. The research reported in this paper was performed in connection with Contract/Cooperative Agreement DAAD17-99-C-0062 with the U.S. Army Research Laboratory.

C. M. DePriest, T. Yilmaz, and P. J. Delfyett are with the School of Optics/Center for Research and Education in Optics and Lasers (CREOL), University of Central Florida, Orlando, FL 32816 USA.

A. Braun and J. Abeles are with David Sarnoff Research Center, Princeton, NJ 08543 USA.

Publisher Item Identifier S 0018-9197(02)02649-0.

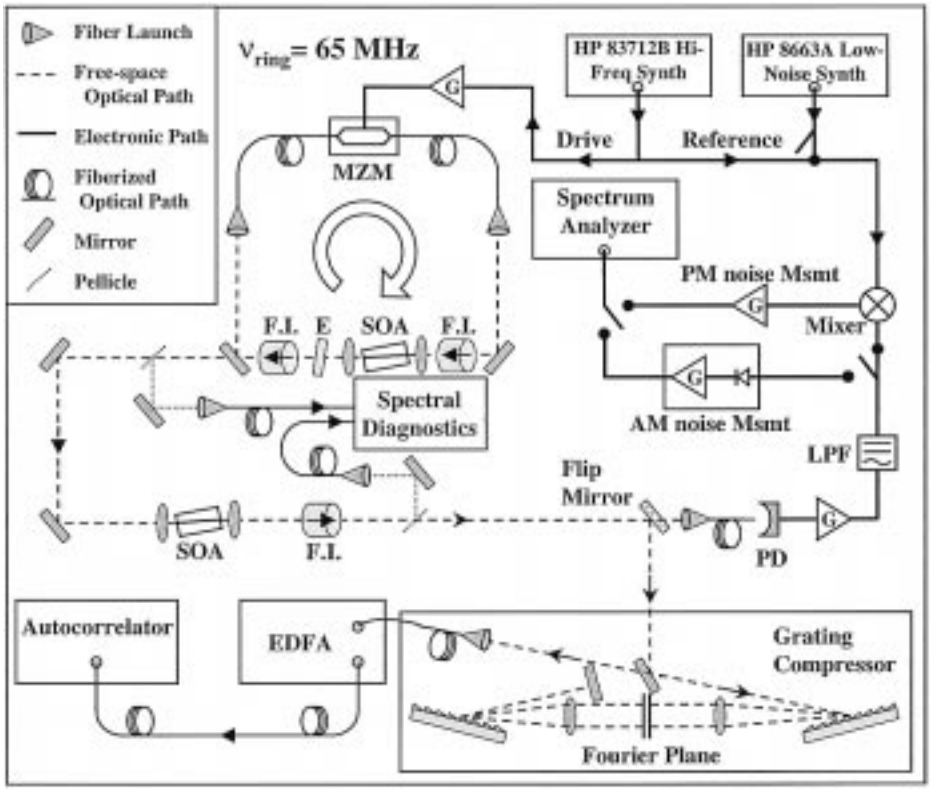

Fig. 1. Experimental layout of ring laser and peripherals. (MZM: Mach–Zehnder modulator, F.I.: Faraday isolator. E: etalon. SOA: semiconductor optical amplifier. PD: 20-GHz high-speed photodiode. LPF: low-pass filter. G: electrical amplifier.)

second SOA provides single-pass amplification, after which the pulsetrain is directed either to a high-speed photodiode (BW $\sim$20 GHz) for noise measurement or to a dual-grating compressor for dispersion compensation/pulsewidth measurement. The $\sim$10 dB of optical loss in the dispersion-compensator necessitates further amplification via EDFA before pulsewidths are measured using a standard SHG autocorrelator.

Modelocking was achieved using two techniques: loss modulation and gain modulation. Loss modulation involved biasing the SOA at 90–120 mA dc (depending on modelocking frequency) while applying a synthesized RF sine wave ($+25$ dBm) to the Mach–Zehnder modulator. Gain-modulated modelocking required a lower dc bias on the SOA (80–95 mA) while the RF signal ($+30$ dBm) was injected into the SOA through a bias tee. Current data consists of actively mode-locked pulse rates as high as 10 GHz using loss modulation, and 1 GHz using gain modulation (the gain-modulated frequency response was limited to 1 GHz by the impedance characteristics of the diode and mount).

Pulsetrain phase-noise results were acquired by mixing the low-pass-filtered fundamental frequency component of the detected optical signal with that of the driving synthesizer (thereby translating the carrier noise sidebands down to baseband) [22]. The noise signals were then amplified and resolved over six decades of offset frequency (10 Hz–10 MHz) with a HP 3585A RF spectrum analyzer. Amplitude noise sidebands were similarly resolved in the frequency domain after being isolated from phase noise through a Shottky-diode detector in a HP 11729C Carrier Noise Test Set. We believe these noise measurements to be accurate to within $\pm$2 dBc (or $\pm$12% in the rms integral).

III. General Survey of Ring Laser Noise

Due to its traveling-wave nature, the unidirectional ring cavity allows easy access to the technique known as harmonic modelocking. In an effort to better understand the laser's noise characteristics, a survey of noise data was compiled at octave intervals of the modelocking frequency, beginning with operation at the second cavity harmonic (130 MHz) and ending with the 128th (8.32 GHz). Two driving synthesizers were used: a low-noise HP 8663A (100 kHz–2.5 GHz), as well as a high-frequency HP 83712B (10 MHz–20 GHz). (The nature of these experiments requires a synthesizer with a wide tuning band. Although several single-frequency oscillators exist that can outperform these sources, we believe that these experiments provide valuable information even when using a less-than-optimal source.) The laser was actively mode-locked using loss modulation, as well as gain modulation, and the effects of the two techniques on pulsetrain noise are compared. Although gain-modulated modelocking of the 2.3-mm SOA was only possible for frequencies up to $\sim$1 GHz due to system-impedance limitations in the instrumentation, some useful insight can nevertheless be gained from the resulting data.

Three classes of noise were investigated: amplitude modulation (AM) noise, as well as both "absolute" and "residual" phase modulation (PM) noise. Absolute PM noise, in this case, is used to refer to the situation in which the laser's detected pulsetrain was referenced to a synthesizer having significantly lower noise characteristics (8663A) than the one driving the laser (83712B). Measurements of absolute PM noise were made only when the 83 712B was providing the laser's driving signal,

since no source was had with significantly lower noise than the 8663A. Residual PM noise refers to a comparison between the detected optical signal and the synthesizer signal actually driving the laser and, therefore, could be measured using both sources. Residual noise represents the phase noise added to the driving signal by the laser cavity. All three noise types were measured over six decades of offset frequency (10 Hz–10 MHz), and the data points in the following figures represent the result of integration over this entire range. The expressions used to calculate rms values for timing jitter and amplitude noise follow from [22] and [23], respectively:

$$\Delta t_j = \frac{1}{2\pi \cdot f_c}\sqrt{2\int_{f_{\rm lo}}^{f_{\rm hi}} L(f)df} \tag{1}$$

$$\frac{\Delta a}{A} = \sqrt{2\int_{f_{\rm lo}}^{f_{\rm hi}} P_A(f)df}. \tag{2}$$

Equation (1) indicates the rms timing jitter Δt_j (in units of seconds) as a function of the RF carrier frequency f_c and the single-sideband phase noise density $L(f)$ (measured relative to the carrier power). Equation (2) indicates the rms amplitude fluctuation, $\Delta a/A$, (units are in percent relative to the average RF carrier power, A) as a function of the single-sideband amplitude noise density, $P_A(f)$. Noise densities in both equations are integrated over offset frequencies between $f_{\rm lo}$ and $f_{\rm hi}$. In Figs. 3 and 4, the results of phase noise integrations are also plotted in relative units (percent of the carrier period, T) so as to normalize the comparison between different modelocking frequencies

$$\frac{\Delta t_j}{T} = \frac{1}{2\pi}\sqrt{2\int_{f_{\rm lo}}^{f_{\rm hi}} L(f)df}. \tag{3}$$

Measurements were performed at 2^n harmonics of the fundamental longitudinal mode spacing in order to provide an efficient means for covering the roughly two decades of interest in this survey. Changes in noise properties over this operating range do not occur rapidly enough to warrant sampling this frequency range in a linear manner. Errors associated with the measurement process are systematic, and therefore common to all data points. As before, we estimate the uncertainty in these data points to be roughly 12% of their stated values.

The results of the noise survey are shown in Figs. 2–4, where the integrated and normalized (units of percent) rms noise is plotted versus modelocking frequency for each combination of driving synthesizer and modelocking method. Figs. 2–4 show the integrated amplitude noise, residual phase noise, and absolute phase noise, respectively, each plotted versus modelocking frequency. In all three plots, the dotted curves with open symbols correspond to loss-modulated modelocking, while the solid curves with solid symbols are the result of gain-modulated modelocking. To distinguish between synthesizers, triangular data points correspond to driving with the high-frequency 83 712B, while the circular data points correspond to driving with the low-noise 8663A.

We begin with an overview of the AM noise results in Fig. 2. The first salient feature of these curves is that all measured data points reside at a significantly higher rms noise level than the AM fluctuations of either driving source directly (see Fig. 6 for an AM noise curve of the 83 712B—the 8663A's curve is comparable). The measured AM noise of the synthesizers is below 0.03% rms, and the minimal data point in Fig. 2 surpasses this value by a factor of ten. This suggests that amplitude noise in the synthesizers plays a relatively minor role in shaping the AM

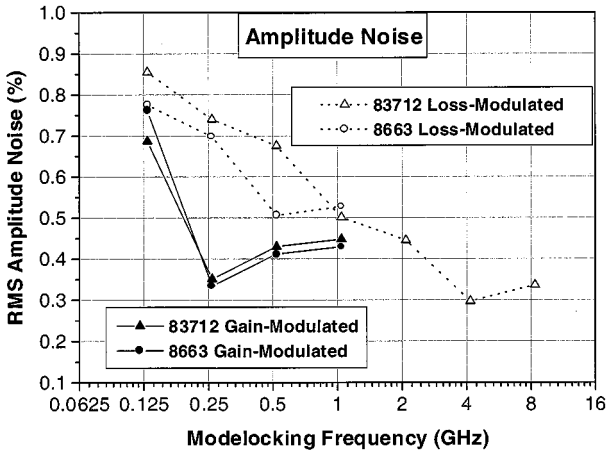

Fig. 2. Integrated rms amplitude noise (10 Hz–10 MHz) versus modelocking frequency for various active modelocking conditions.

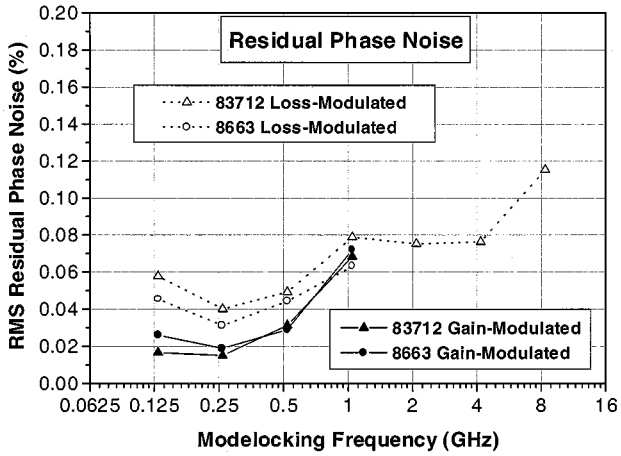

Fig. 3. Integrated rms residual phase noise (10 Hz–10 MHz) versus modelocking frequency for various active modelocking conditions.

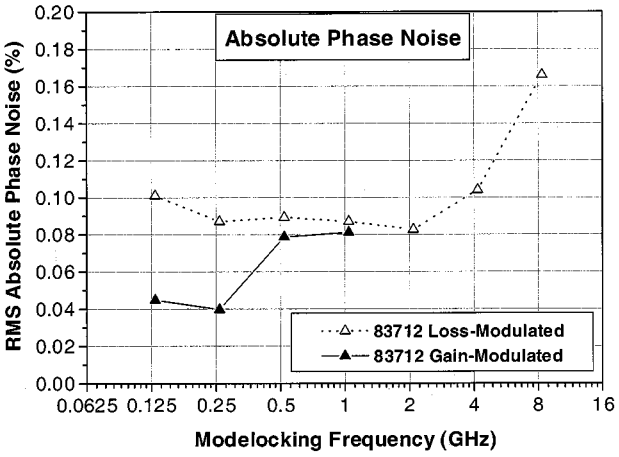

Fig. 4. Integrated rms absolute phase noise (10 Hz–10 MHz) versus modelocking frequency for various active modelocking conditions (data measured only while driving with 83 712B high-frequency synthesizer).

noise of the mode-locked pulsetrains. This suggestion was confirmed by amplitude-modulating the laser driving signal to produce AM sidebands, and then observing the resulting sidebands in the photodetector signal. The relative strength (dBc) of the modulation sidebands in the laser signal was seen to have decreased by slightly more than 10 dBc compared to those in the driving signal.

A more interesting feature in Fig. 2 is the noticeable difference in the AM noise associated with the distinct modelocking techniques (gain versus loss modulation). Loss-modulated modelocking is seen to produce a steady decrease ($\sim$0.1% per octave) in AM noise with increasing drive frequency. Gain-modulated modelocking, on the other hand, exhibits a more complicated trend: beginning with slightly lower numbers at 130 MHz, the noise then drops significantly at the next octave, turns slowly upward, and appears to begin merging with the loss-modulated data as 1 GHz is approached. This advantage of gain-modulated modelocking is exhibited in all of the types of noise investigated. Another characteristic common to all noise trends is the upward discontinuity observed in the final octave of modelocking frequency (the transition from 4.15 to 8.3 GHz shows a larger jump than would be expected based on the data's previous trend). Finally, note that the loss-modulated data associated with the lower-noise synthesizer (8663A) falls slightly below that of the 83 712B—as will be discussed shortly, the residual phase noise displays the same behavior. The gain-modulated data, however, does not show a noticeable deviation between synthesizers.

Residual PM noise measurements are compiled in Fig. 3 (rms units are in percentage of modelocking period). This data reveals a general trend toward *increasing* noise with modelocking frequency. The lower noise achieved using gain modulation is still present, as is the trend toward convergence between modelocking techniques as the driving frequency approaches 1 GHz. Loss modulation again displays a noticeable offset between synthesizers while gain modulation does not. Finally, the significant discontinuity in the last octave of the loss-modulated data is also observed.

Absolute PM noise measurements are compiled in Fig. 4. (Since these measurements, by definition, required a reference synthesizer with significantly lower-noise than the one driving the laser, no measurements were made when using the 8663A for modelocking.) These rms values are slightly higher than the corresponding residual noise values, as expected. Gain and loss modulation again display their characteristic differences, as well as their convergence as 1 GHz is approached. The discontinuity in the last octaves of loss modulation is also observed.

Beginning the discussion with AM noise (Fig. 2), several comments can be made regarding these results. Spontaneous emission is targeted as the primary contributor to pulsetrain noise in several theoretical papers [24]–[26]. Success in lowering the amount of spontaneous emission being coupled into extraneous (nonlocked) longitudinal modes of the cavity would, therefore, be expected to have positive consequences. The most general tendency observed in Fig. 2 is the overall decrease in AM noise with increasing modelocking frequency. We believe this to be a consequence of the increase in average pulsetrain power as well as the decrease in pulsewidth that both accompany modelocking at higher frequencies. Over the measured modelocking range, pulsetrain power is observed to change from $\sim$3 mW at 130 MHz to $\sim$20 mW at 8.3 GHz, while the measured pulsewidth changes from $\sim$22 to $\sim$27 ps (for corresponding frequencies). The increase in average power will tend to increase the more fundamental signal-to-noise ratio determined by statistical fluctuations (since smaller statistical noise is known to accompany a larger photon population). In addition, the fact that the ratio of pulsewidth to modelocking period becomes larger (2.9% at 130 MHz to 22.4% at 8.3 GHz) will tend to reduce the percentage of the period occupied by (noisy) spontaneous emission. (The majority of a well-formed pulse's photon population resides within a relatively narrow optical band.) These effects lower the overall ratio of average spontaneous emission power to average pulsetrain power, and most likely contribute to the observed decrease in AM noise that occurs with increasing modelocking frequency.

Another aspect to notice in Fig. 2 is that the AM noise associated with the gain-modulated laser is generally lower than that of the loss-modulated laser. As the pulse passes through the homogeneous gain medium of the diode, photons are primarily stimulated into a relatively narrow optical band, while the random spontaneous emission is temporarily quenched. After the pulse leaves the gain medium, the ASE then increases in accordance with the gain recovery time (in the case of loss modulation) or with the pumping rate (in the case of gain modulation). In the loss-modulated case, the ASE emitted between pulses is reasonably constant since the diode is dc biased. Gain modulation, on the other hand, tends to intrinsically decrease the amount of ASE between pulses by effectively shutting off the pumping rate. We attribute the generally better AM noise performance exhibited by gain modulation to the superior manner in which the interpulse ASE is quenched.

A final focus of discussion is the way in which the AM noise of both modelocking methods is seen to converge at higher pulse rates. We believe this to be due to the empirical fact that the dc-component of the drive current used in gain-modulated modelocking must be increased with pulse rate in order to retain a quality mode-locked pulsetrain. At lower modelocking rates, the average (dc) level of driving current can be placed well below the threshold current of the laser, resulting in a narrower time window for pulse formation (relative to the modelocking period), as well as an increased window of spontaneous emission quenching over the remainder of the driving cycle. This is in contrast to the dc bias when modelocking with loss modulation, which must always remain above the laser's threshold. As the gain-modulated modelocking rate increases, however, it becomes necessary for optimal performance to increase the dc bias on the diode. This then increases the ASE between pulses, and therefore causes gain modulation to lose its advantage over loss modulation.

Residual phase noise exhibits an opposite trend compared to amplitude noise—appearing to increase with modelocking frequency. We believe this behavior to be associated with a decrease in the energy per pulse as the modelocking frequency increases, which subsequently tends to relax the opposing nonlinear mechanisms that stabilize the positions of each pulse in the time domain. For example, variations in dynamic gain saturation tend to advance the pulse in time, while variations in dy-

namic index tend to retard the pulse in time [26]. The efficiency of such nonlinear mechanisms decreases with pulse energy. The end result produced by an increase in the pulse repetition rate, then, would be a relaxation of the locking constraints that keep the pulses anchored in the time domain. One can, therefore, expect a larger variation (noise) in the stabilized variable (time) and, hence, an increase in the pulse-to-pulse jitter.

An interesting observation in Figs. 2 and 3 is that the loss-modulated laser shows slightly lower amplitude noise and residual jitter when being driven with the synthesizer having the lower phase noise. Residual phase noise, by definition, is a measure of the noise added by the laser, and is theoretically independent of the level of noise in the driving synthesizer. The fact that this trend is observed in the AM noise as well, even though the AM noise of the two driving synthesizers is well below that of the laser, is also interesting. These results suggests two interesting possibilities for the loss-modulated geometry: 1) enhanced AM–PM noise coupling (compared to gain modulation) and 2) increasing residual phase noise with increasing source phase noise. Loss-modulated modelocking was accomplished through the use of a Mach–Zehnder modulator, which uses the Pockels effect to convert changes in optical index into changes in optical amplitude. This could provide a somewhat stronger mechanism for AM–PM coupling than what exists in a gain-modulated system, since an instantaneous phase change of the driving signal (absolute PM) will impress a new voltage on the modulator in time. This may lead to changes in the pulse intensity as well as its position. The gain modulated curves, on the other hand, do not show as noticeable an offset between synthesizers, in either AM or residual PM noise. The "residual" nature of phase noise seems more preserved with gain modulation, in accordance with the fairly minor AM–PM coupling mechanisms that are predicted theoretically [26].

The laser's absolute phase noise in Fig. 4 shows the familiar contrast between gain and loss modulation. The noise of the 83 712B synthesizer is known to increase with operating frequency, which explains the general trend in Fig. 4 (as gain modulation was seen to produce significantly lower residual noise in Fig. 3, its absolute noise, by definition, more closely matches that of the synthesizer at lower frequencies). However, the deviation of the data over the last two octaves is quite significant. Such a deviation suggests an important change in the laser dynamics at higher modelocking frequencies (specifically between 4 and 8 GHz). This transition is believed to be related to the resonance associated with the relaxation oscillation, which falls within this frequency range.

IV. Ultralow-Noise Optical Sampling Streams

The low-noise requirements of optical sampling systems become increasingly more difficult to attain as the goals associated with either sampling frequency or bit resolution become more assertive [17]. If performing the sampling with optical pulsetrains, a decrease in pulsewidth must also accompany higher bit rates [6]. We have experimentally investigated the ability of actively mode-locked external-cavity semiconductor diode lasers to meet these requirements, and it is the operating characteristics of our 10-GHz ring laser that will now be presented.

The attributes of our 10-GHz loss-modulated ring laser were investigated using two different geometries. Since earlier experimental results suggested the tendency for noise to increase as the laser is operated with more optical bandwidth [21], lowest noise operation was initially achieved by incorporating a band-limiting etalon ($\sim$7-nm FSR, finesse $\sim$5) into the cavity. Shortest pulse operation required the removal of the etalon to allow the mode-locked bandwidth to broaden considerably. Careful tuning of the modelocking conditions then facilitated the organization of a highly linear chirp [27], which allowed the pulsewidth to be compressed by a factor of $\sim$10 through the use of a dual-grating dispersion compensator. It was seen that the shortest pulse geometry causes only a slight increase in laser phase noise, but a more appreciable increase in laser amplitude noise.

A restriction appropriate to the type of pulsed optical sampling system described here involves the width of the sampling pulses. Taylor has presented an argument for the maximum pulse interaction time allowed when trying to optically sample a signal of bandwidth $\nu_{\rm sig}$ while retaining an accuracy of N bits [6]. For a system sampling at the Nyquist frequency, this argument is based on the need to reduce pulse amplitude errors to less than $1/2$ least-significant-bit (LSB) for an input signal covering the full peak-to-peak amplitude range. When amplitude-modulating an optical pulsetrain as it passes through a velocity-matched Mach–Zehnder intensity modulator, it would be appropriate to assume a gaussian (rather than rectangular) sampling window. Applying this minor revision to Taylor's argument results in the following requirement on the sampling pulsewidth t_p (FWHM)

$$t_p \leq \frac{2\sqrt{\ln 2}}{\pi \cdot \nu_{\rm sig}} \sqrt{\frac{1}{2^N}}. \tag{4}$$

This equation, for example, predicts the need for 1.7-ps pulsewidths in order to sample a 5-GHz signal at the Nyquist rate with 12 bits of resolution.

Fig. 5 compares the temporal autocorrelations and mode-locked optical spectra of the 10-GHz laser when operating both with and without the intracavity etalon. The laser's pulsewidth is seen to decrease from 13 to 1.2 ps (after dispersion compensation), while the mode-locked spectral width increases from 0.47 to 5.1 nm. The time-bandwidth product under both conditions remained the same: $\sim$1.7 times transform-limited. According to (4), the narrow-band pulses (13 ps) would allow a resolution of only 2 bits for sampling a 5-GHz signal at the Nyquist frequency, while as many as 12.9 bits of resolution are possible using the 1.2-ps pulses.

The measured AM noise sidebands of the 10-GHz laser (both in narrow-and wide-band operation) are shown in Fig. 6, along with the AM noise of the driving synthesizer (83712B). The noise curve for wideband laser operation (without the etalon) possesses a "knee" at approximately 500-kHz offset. It is believed that this characteristic is due to a well-defined photon correlation time that results from both the cavity roundtrip time and cavity Q [26]. This knee may become washed out (decorrelated) when the etalon is commissioned because a new and unrelated time constant has been added to the resonator. Integration of these noise sidebands over the entire displayed offset

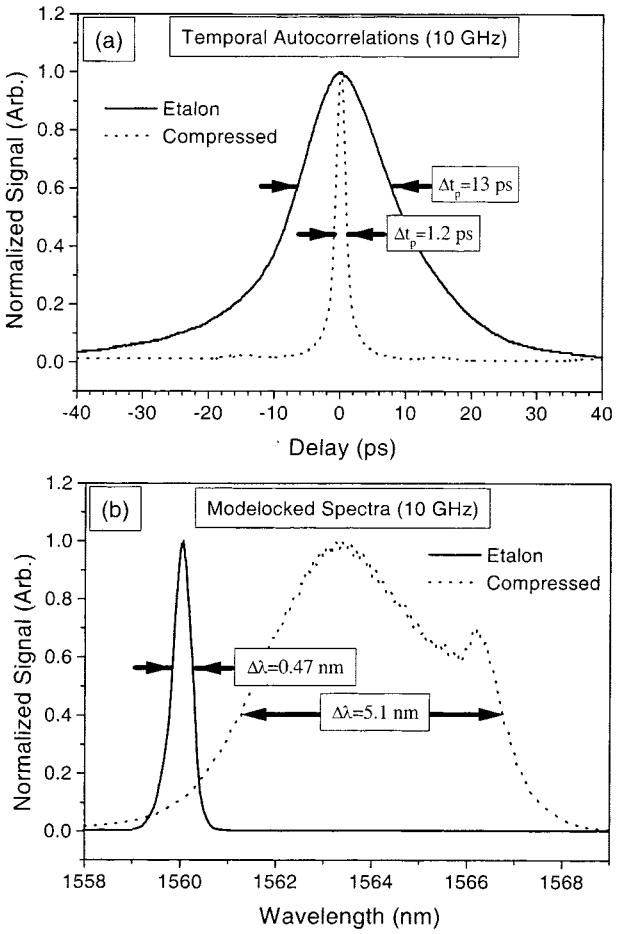

Fig. 5. (a) Temporal autocorrelations and (b) mode-locked spectra for laser operation with and without intracavity etalon (short pulse resulting from spectral dispersion compensation on wideband mode-locked spectrum).

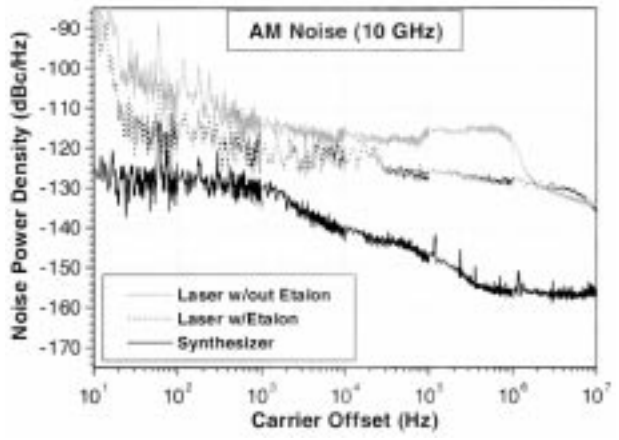

Fig. 6. Mode-locked (10 GHz) pulsetrain amplitude noise sidebands for narrowband and wideband laser operation compared to synthesizer AM noise.

range (10 Hz–10 MHz) results in a rms amplitude fluctuation of 0.27% without the etalon, and 0.12% with the etalon.

In order to estimate the ADC conversion accuracy associated with these results, we must integrate the noise curves out to the Nyquist frequency. We assume a continuance of the downward slope that exists in the curves of Fig. 6 (beyond the knee), and regard the fundamental noise floor to be −159 dBc/Hz (this being

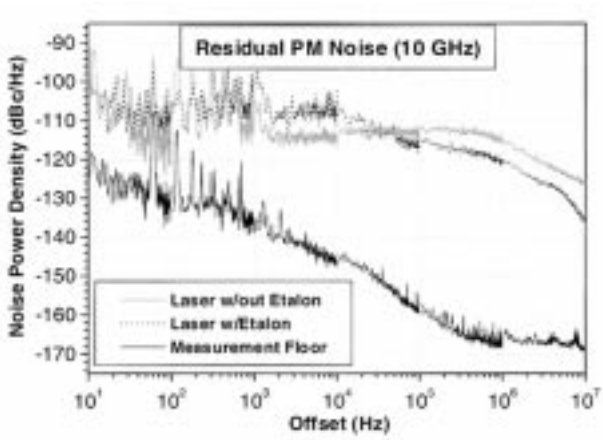

Fig. 7. Mode-locked (10 GHz) residual phase noise sidebands for narrowband and wideband laser operation, along with residual phase noise measurement floor.

the shot noise limit associated with our 20-mW pulsetrain [28]). Using these assumptions, integrating out to the Nyquist offset (5 GHz) results in total rms fluctuations of 0.21% and 0.33% (with and without the etalon, respectively).

Now we identify the most-significant-bit (MSB) with the amplitude of the carrier, and demand that the rms AM fluctuation correspond to a value less than one-half of the LSB. Such an argument applied over the displayed frequency range suggests a theoretical resolution of 7.9 and 7.3 bits, respectively, for operation with and without the etalon, respectively. Because amplitude fluctuations are independent of the laser sampling rate, this result is also independent of modelocking frequency.

The laser's residual PM noise sidebands are shown in Fig. 7, along with the residual noise measurement floor. (The noise floor was obtained by referencing the driving signal to itself, and thus represents the amount of noise contributed by the mixer and amplifier used in the measurement system.) The phase noise here is referred to as "residual" due to the fact that the detected laser signal was compared to that of the driving synthesizer, thereby measuring the amount of phase noise added by the laser itself [22]. The knee characteristics are seen to closely resemble those in the AM noise curves (the comparatively well-defined wideband knee becomes washed out during narrowband operation). Integration of the PM noise curves in Fig. 7 over all displayed frequency offsets gives a rms jitter of 48 fs for the wideband system and 43 fs for the narrow-band system.

Extended integrations of these curves out to the Nyquist frequency (using the same assumptions outlined above for the case of AM noise) result in total rms jitters of 52 and 114 fs for operation with and without the etalon, respectively. Using Walden's result relating equivalent theoretical bit resolution, N to rms jitter τ_j, [17] as follows:

$$N = \log 2 \left(\frac{2}{\sqrt{3}\pi \cdot f_{\text{samp}} \tau_j} \right) - 1 \tag{5}$$

one finds that these levels of phase noise would be sufficient to resolve 8.5 and 7.3 bits, respectively, at a Nyquist sampling rate of 10 GHz.

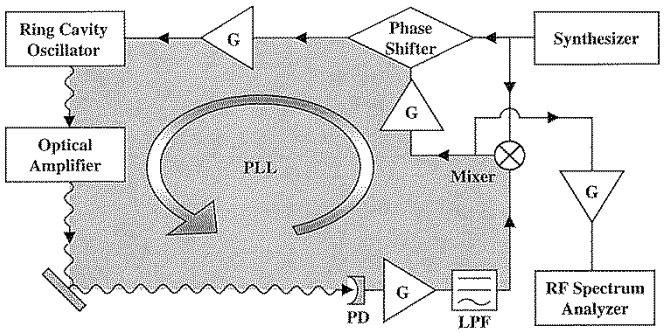

Fig. 8. Schematic of 2-GHz phase-locked-loop for residual phase noise reduction. (G: electrical amplifier. LPF: low-pass filter. PD: 20-GHz photodiode detector).

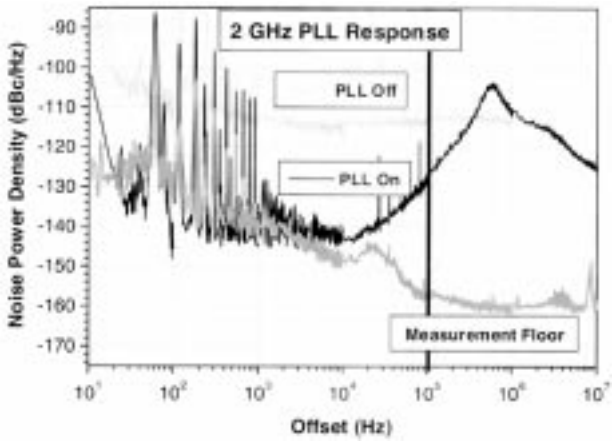

Fig. 9. Residual phase noise reduction by PLL in mode-locked laser pulsetrain (2 GHz) showing phase noise reduction out to 100-kHz offsets.

The complexity with which noise causes and effects are related in this system has motivated a proof-of-principle attempt at reducing laser noise using an empirical strategy: the phase-locked-loop (PLL). Our implementation of this device consisted of a commercial mixer, a commercial voltage-controlled phase shifter, and a home-built amplifier arranged in a negative-feedback geometry designed to promote closer phase tracking of the driving source by the laser (Fig. 8). Voltage-controlled phase shifters are currently offered in rather limited variety for use with multigigahertz carriers. The commercial unit that had the widest analog response bandwidth was designed for use on a 2-GHz carrier frequency, which required the laser to be mode-locked at the 31st harmonic.

Results of the 2-GHz locking test are shown in Fig. 9. The three curves represent the laser's residual PM noise under normal operation, the noise of the laser being reduced through PLL action, and the measurement system noise floor. By phase-locking the laser to the driving signal, residual PM noise was reduced by almost 30 dB within the response band of the phase shifter. By integrating the noise sidebands within the PLL response band (out to $\sim$100 kHz—the dark vertical line in Fig. 9), one finds that this in-band rms noise has been reduced by 91% from 88 to 8 fs.

This demonstration shows that the residual phase noise can be substantially reduced ($\sim$30 dB) by purely electronic means (as compared to conventional methods using electro-mechanical means, e.g., piezoelectric transducers). The potential of employing voltage-controlled phase shifters operating on higher carrier frequencies (10 GHz) and having correspondingly larger response bandwidths is undeniable. Using such a device, the bandwidth of the phase locked loop can be pushed beyond the knee or roll-off frequency, resulting in a RPM noise spectrum having a phase noise floor of -140 dBc/Hz over the entire frequency offset range (10 Hz to 5 GHz). This would reduce the pulsetrain phase noise significantly below the 43 fs reported previously.

V. Noise Measurements at Large Offset Frequency

Measured carrier noise spectral densities have traditionally been confined to relatively narrow bands of offset frequency, the limitations being determined primarily by restrictions in the measurement electronics. In an ideal attempt to measure rms noise based on a spectral scan, however, one would like to characterize a continuous-wave source over an infinitely long time period, with infinitely fine temporal resolution, so as to capture both the lowest-and highest-frequency components in the noise. Practicality requires a compromise on these ideals.

The lower cutoff of offset frequency (where to begin the integration) can be chosen based on the amount of time one is willing to spend making the noise measurement. This time interval represents the lowest frequency over which any changes in signal can be detected. The upper cutoff is a different matter. A periodic process such as an optical pulsetrain is composed of several Fourier components, each of which is readily marked in the frequency domain. Noise sidebands associated with the fundamental carrier (or any carrier harmonic, for that matter) can only be distinguished out to the Nyquist offset frequency. Beyond this offset, the noise energy of adjacent harmonics begins to surpass that of the harmonic in question. For this reason, the Nyquist frequency serves as a distinctive barrier between any particular harmonic and it's nearest neighbor. Noise fluctuations beyond this frequency offset can no longer be ascribed to the particular carrier under scrutiny. It is for these reasons that we have attempted the first measurements of noise spectral density out to Nyquist frequency offsets for our 10-GHz laser system.

Fig. 10 displays the noise sidebands of the (broadband) 10-GHz ring laser measured out to the Nyquist offset. Three separate amplifiers were used to boost the noise power after carrier mixing in order to cover the offset range of interest. The plotted curves represent the laser's residual PM noise (dotted), an "effective" noise floor that will be explained shortly (gray), and the ultimate noise floor of our measurement system (black). The spikes occurring over the last three decades are associated with longitudinal supermode beating, which has been ignored in the integration, owing to unresolved issues as to whether these components primarily effect AM or PM noise. It should be noted in any case that the suppression of supermode noise to -140 dBc/Hz has recently been demonstrated [29], which justifies its lack of inclusion in the noise integration.

Integration of the laser's noise curve over all displayed frequencies results in an upper bound on the rms jitter of 121

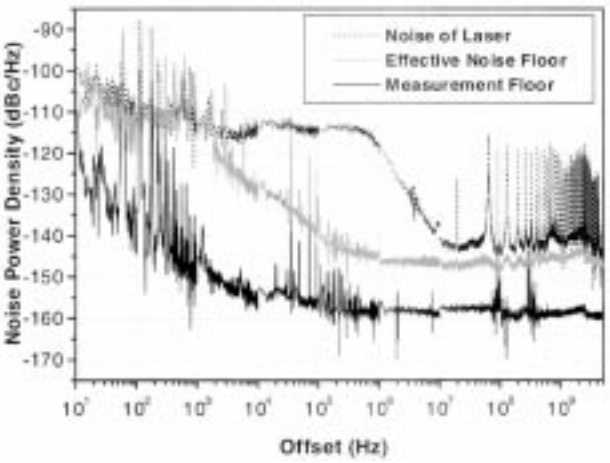

Fig. 10. Residual phase noise measured to Nyquist offsets for 10-GHz mode-locked pulsetrain.

fs. Such a value of pulsetrain jitter would theoretically provide 7.2 bits of resolution.

Beyond offset frequencies of 10 MHz, the measured noise displays a white characteristic. This observation invites a new kind of speculation—does this noise truly represent the laser's behavior, or is it a result of limitations in measurement? The fact that the spikes due to longitudinal mode beating possess peak values in excess of 20-dB above the white noise floor lends a certain amount of validity to their numbers, but the level of the white noise floor itself must be scrutinized. The average power in the 10-GHz fundamental of the signal immediately after photodetection was measured to be roughly -20 dBm. This resides $\sim$153-dB above thermal noise at room temperature. If one assumes that no significant noise figures exist within the detection/measurement system, then this would represent the maximum dynamic range that can be achieved in the phase noise measurement (153 dBc). The measured white noise floor in the phase noise of the laser resides at -145 dBc, only 8-dB above this thermal limit (an amount that could easily be attributed to amplifier noise figures or conversion loss in the mixer). In an effort to confirm this empirically, a measurement was arranged to simulate the expected "experimental" noise floor. Two identical synthesizer signals at $\sim$0 dBm are normally used to test the residual noise measurement floor (black curve in Fig. 10). If one of these signals is first attenuated to the level of the photodetector output $(-20$ dBm$)$ and then sent through the same RF amplifier that is used to experimentally boost the detector signal, an "effective" residual noise measurement floor that is more representative of the experimental conditions will be measured. The result of such a measurement is a greatly compromised "effective" noise floor (gray curve). In fact, the effective white noise floor in Fig. 10 resides only 5 dB below the measured laser noise. This implies a strong possibility that the displayed laser noise floor is due to measurement limitations rather than the laser itself, and tends to bring the validity of the total rms jitter quoted earlier into question. It is for this reason that the measured value of 121 fs is referred to as an upper bound.

VI. Conclusion

We have presented an external-cavity, actively mode-locked semiconductor diode ring laser capable of extremely high stability. Gain modulation was found to produce mode-locked pulsetrains with better noise characteristics at lower driving frequencies due to a more efficient quenching of intracavity spontaneous emission. Mode-locked pulsetrains at 10 GHz exhibited pulsewidths as low as 1.2 ps, amplitude noise as low as 0.12% rms (10 Hz–10 MHz), and residual phase noise jitter as low as 43-fs rms (10 Hz–10 MHz). The stability of these sampling streams would provide a resolution of $\sim$8 bits in a photonic analog-to-digital converter sampling at 10 GHz. A proof-of-principle reduction of in-band (10 Hz–100 kHz) rms phase noise by as much as 91% was accomplished through implementation of a home-built phase-locked-loop. Finally, the measurement of high-frequency laser phase-noise out to the Nyquist offset has been accomplished for the first time at a 10-GHz carrier frequency, resulting in an upper limit of rms jitter of 121 fs (10 Hz–5 GHz).

References

[1] P. J. Delfyett, D. H. Hartman, and S. Z. Ahmad, "Optical clock distribution using a mode-locked semiconductor laser diode system," *IEEE J. Lightwave Technol.*, vol. 9, pp. 1646–1649, 1991.

[2] C. Baringer, J. F. Jensen, L. Burns, and R. H. Walden, "A 3-bit, 8 GSPS flash ADC," in *Proc. Indium Phos. Rel. Mater. Conf. 1996*, New York, 1996, pp. 64–67.

[3] P. Xiao, K. Jenkins, M. Soyuer, H. Ainspan, J. Burghartz, H. Shin, M. Dolan, and D. Harame, "A 4b 8GSample/s A/D converter in SiGe bipolar technology," in *Proc. IEEE Int. Solid-State Circuits Conf.*, New York, 1997, pp. 124–125.

[4] S. B. Kaplan, P. D. Bradley, D. K. Brock, D. Gaidarenko, D. Gupta, W. Li, and S. V. Rylov, "A superconductive flash digitizer with on-chip memory," *IEEE Trans. Appl. Superconduct.*, vol. 9, pp. 3020–3025, 1999.

[5] D. H. Auston, "Picosecond optoelectronic switching and gating in silicon," *Appl. Phys. Lett.*, vol. 26, pp. 101–103, 1975.

[6] H. F. Taylor, "An optical analog-to-digital converter—Design and analysis," *IEEE J. Quantum Electron.*, vol. QE-15, pp. 210–216, 1979.

[7] J. A. Valdmanis, G. Mourou, and C. W. Gabel, "Picosecond electro-optic sampling system," *Appl. Phys. Lett.*, vol. 41, pp. 211–212, 1982.

[8] R. A. Becker, C. E. Woodward, F. J. Leonberger, and R. C. Williamson, "Wide-band electrooptic guided-wave analog-to-digital converters," *Proc. IEEE*, vol. 72, pp. 802–819, 1984.

[9] T. Kanada and D. L. Franzen, "Optical waveform measurement by optical sampling with a mode-locked laser diode," *Opt. Lett.*, vol. 11, pp. 4–6, 1986.

[10] P. E. Pace, S. J. Ying, J. P. Powers, and R. J. Pieper, "Integrated optical sigma–delta modulators," *Opt. Eng.*, vol. 35, pp. 1828–1836, 1996.

[11] T. R. Clark, J. U. Kang, and R. D. Esman, "Performance of a time-and wavelength-interleaved photonic sampler for analog-digital conversion," *IEEE Photon. Technol. Lett.*, vol. 11, pp. 1168–1170, 1999.

[12] A. Johnstone, M. F. Lewis, J. D. Hares, and P. A. Kellett, "High-speed opto-electronic transient waveform digitizer," in *Proc. 3rd Int. Conf. Advanced A/D and D/A Conversion Techniques and Their Applications*, New York, 1999, pp. 21–24.

[13] E. N. Toughlian and H. Zmuda, "A photonic wide-band analog to digital converter," in *Int. Topical Mtg. Microwave Photonics*, 2000, pp. 248–250.

[14] A. S. Bhushan, P. Kelkar, and B. Jalali, "30 Gsample/s time-stretch analogue-to-digital converter," *Electron. Lett.*, vol. 36, pp. 1526–1527, 2000.

[15] P. Rabiei and A. F. J. Levi, "Analysis of hybrid optoelectronic WDM ADC," *IEEE J. Lightwave Technol.*, vol. 18, pp. 1264–1270, 2000.

[16] M. Johansson, B. Löfving, S. Hård, L. Thylén, M. Mokhtari, U. Westergren, and C. Pala, "Study of an ultrafast analog-to-digital conversion scheme based on diffractive optics," *Appl. Opt.*, vol. 39, pp. 2881–2887, 2000.

[17] R. H. Walden, "Analog-to-digital converter survey and analysis," *IEEE J. Select. Areas Commun.*, vol. 17, pp. 539–550, 1999.
[18] C. M. DePriest, A. Braun, J. Abeles, and P. J. Delfyett Jr., "10-GHz ultralow-noise optical sampling stream from a semiconductor diode ring laser," *IEEE Photon. Technol. Lett.*, vol. 13, pp. 1109–1111, 2001.
[19] H. Shi, J. Finlay, G. A. Alphonse, J. C. Connolly, and P. J. Delfyett, "Multiwavelength 10-GHz picosecond pulse generation from a single-stripe semiconductor diode laser," *IEEE Photon. Technol. Lett.*, vol. 9, pp. 1439–1441, 1997.
[20] E. Park, P. J. Delfyett, and J. H. Abeles, "Multi-wavelength generation at 1.55 μm from an external cavity semiconductor laser," *Proc. SPIE*, vol. 4042, pp. 82–90, 2000.
[21] H. Shi, I. Nitta, G. A. Alphonse, J. C. Connolly, and P. J. Delfyett, "Timing jitter performance of multiwavelength modelocked semiconductor laser," *Electron. Lett.*, vol. 34, pp. 1–2, 1998.
[22] D. J. Derickson, A. Mar, and J. E. Bowers, "Residual and absolute timing jitter in actively modelocked semiconductor lasers," *Electron. Lett.*, vol. 26, pp. 2026–2028, 1990.
[23] D. von der Linde, "Characterization of the noise in continuously operating mode-locked lasers," *Appl. Phys. B.*, vol. 39, pp. 201–217, 1986.
[24] P.-T. Ho, "Phase and amplitude fluctuations in a mode-locked laser," *IEEE J. Quantum Electron.*, vol. QE-21, pp. 1806–1813, 1985.
[25] D. R. Hjelme and A. R. Mickelson, "Theory of timing jitter in actively mode-locked lasers," *IEEE J. Quantum Electron.*, vol. 28, pp. 1594–1605, 1992.
[26] F. Rana and R. Ram, "Timing jitter and noise in mode-locked semiconductor lasers," presented at the Conference on Electro-Optics and Lasers, 2001, paper CMB2.
[27] A. S. Hou, R. S. Tucker, and G. Eisenstein, "Pulse compression of an actively modelocked diode laser using linear dispersion in fiber," *IEEE Photon. Technol. Lett.*, vol. 2, pp. 322–324, 1990.
[28] B. E. A. Saleh and M. C. Teich, *Fundamentals of Photonics*. New York: Wiley, 1991, pp. 673–677.
[29] C. M. DePriest, T. Yilmaz, S. Etemad, A. Braun, J. Abeles, and P. J. Delfyett Jr., "Ultralow noise and supermode suppression in an actively-modelocked external-cavity semiconductor diode ring laser," *Opt. Lett.*, submitted for publication.

Christopher M. DePriest received the B.S. degree in physics from the University of Texas at Austin in 1993 and the M.S. degree in applied physics from the University of North Carolina at Charlotte in 1996. He is currently working toward the Ph.D. degree in optical physics at the School of Optics/CREOL, University of Central Florida, Orlando.

His current research interests include applications of external-cavity semiconductor diode lasers, ultralow-noise optical pulsetrain generation, and the use of optical techniques in pulsetrain noise measurement.

Mr. DePriest is a member of the IEEE LEOS Society, the Optical Society of America, and the International Society for Optical Engineering (SPIE).

Tolga Yilmaz received the B.S. degree in physics from the Bilkent University, Bilkent, Turkey in 1996, and the M.S. degree in physics from Indiana University at Bloomington in 1997. He is currently working toward the Ph.D. degree in optics at the School of Optics/CREOL, University of Central Florida, Orlando.

His current research interests include applications of external-cavity semiconductor diode lasers, ultralow-noise pulsetrain generation with optical frequency stabilization, and optical sampling techniques.

Mr. Yilmaz is a member of the IEEE LEOS Society and the International Society for Optical Engineering (SPIE).

Alan Braun received the B.S. (E.E.) degree from Lehigh University, Lehigh, PA, in 1990 and the Ph.D. degree in electrical engineering from The University of Michigan at Ann Arbor in 1997. His dissertation research included the development of diode-pumped ultra-short pulse laser systems, as well as the study of self-trapped propagation of high-peak-power laser pulses through air.

He conducted a one-year Postdoctoral Fellow position concentrating on high-power optical parametric amplifiers at the Laboratoire d'Optique Appliquee, Ecole Polytechnique, Palaiseau, France. In 1998, he joined Sarnoff Corporation, Princeton, NJ, as a Member of the Technical Staff within the Optoelectronics Business Unit. He has worked on developing and characterizing various laser systems employing internally developed optoelectronic devices. His main activity centers on the development of low-noise external-cavity semiconductor mode-locked laser sources. Further, he has developed a linewidth and RIN measurement test-bed for use in characterizing high-power DFB lasers and has been investigating numerically the spectral and temporal characteristics of various resonate optical filters.

Dr. Braun is a member of the Optical Society of America.

Joe Abeles received the B.S. degrees in physics and electrical engineering from Massachusetts Institute of Technology, Cambridge, MA, in 1976, and the M.A. and Ph.D. degrees in physics from Princeton University, Princeton, NJ. He also attended the Karyn Kupcinet International Science Summer School, Weizmann Institute of Science, Rehovot, Israel, in 1978, analying heavy ion-scattering at the Tevatron accelerator.

Currently, he is Head of Photonic ICs and Components in the Optoelectronics and Integrated Systems Business Unit, Sarnoff Corporation, Princeton, NJ, which he joined in 1989. He is responsible for demonstrations and innovations in a variety of single-wavelength and dynamically single-wavelength-distributed feedback and distributed Bragg reflector diode lasers such as coupled-cavity InGaAlP, short-wavelength InAlGaAs, and high-power InGaAsP devices, as well as the first demonstration of a monolithic integrated tapered-amplifier master-oscillator-power-amplifier laser, in the form of a grating-surface-emitting laser in 1992. He co-founded Princeton Lightwave, Inc., Cranbury, NJ in 2000, and has advised in the creation of several other photonics companies. He is active in customer interactions and in the recruitment of technical staff to Sarnoff. He is an inventor of the broadened waveguide material structure, adopted industry-wide for commercial high power diode lasers, and has played a key role in the development of compact mode-locked lasers based on diode gain elements, and in the conceptualization and demonstration of microresonators based on InP and related compounds. He has presented related findings at numerous workshops and conferences on an invited basis. Past contributions at Sarnoff comprise plasma display numerical simulation, phosphors for security applications, high-efficiency visible imager chips, and all-optical computation. From 1982 to 1989, he was with Bell Laboratories, Murray Hill, NJ, and Bellcore, Red Bank, NJ, where he led or collaborated in the invention and development novel high-speed transistors, optical modulators, lasers, and detectors. He participated in the NATO Advanced Study Institute on Submicron Transport in Semiconductors, San Miniato al Monte, Italy, in 1983. He has over 100 publications and holds 14 U.S. patents. He serves on the Advisory Board for the Princeton Opto-Electronics Materials Center. His current research includes integrated photonic circuits for telecommunications, RF applications of photonics, meso-optic and subwavelength photonics, amorphous semiconductor planar lightguide circuits, microfluidic atomic clocks, nanomutated III-Vs, solid-state lighting, photonics business and investment strategy, and U.S. technology interests and policy.

Dr. Abeles has served on Technical Program Committees or as Editor for the Conference on Lasers and Electro-Optics, the Applied Optics Patents Review Panel, the JOURNAL OF LIGHTWAVE TECHNOLOGY, the Optical Society of America Annual Meeting, the International Semiconductor Laser Conference, and the Sarnoff Symposium. He is past Chairman of the IEEE Lasers and Electro-Optics Society's Princeton Chapter.

Peter J. Delfyett, Jr., received the B.E.(E.E.) degree from The City College of New York in 1981, the M.S. degree in electrical engineering from The University of Rochester, Rochester, NY, in 1983, and the M.Phil. and Ph.D. degrees from The Graduate School and University Center of the City University of New York in 1987 and 1988, respectively. His Ph.D. dissertation focused on developing a real-time ultrafast spectroscopic probe to study molecular and phonon dynamics in condensed matter using optical phase-conjugation techniques.

He joined Bell Communication Research, Red Bank, NJ, as a member of the Technical Staff, where his efforts concentrated on generating ultrafast high-power optical pulses from semiconductor diode lasers for applications in applied photonic networks. Some of his technical accomplishments include the development of the world's fastest, most powerful mode-locked semiconductor laser diode, the demonstration of an optically distributed clocking network for high-speed digital switches and supercomputer applications, and the first observation of the optical nonlinearity induced by the cooling of highly excited electron-hole pairs in semiconductor optical amplifiers. While at Bellcore, he received numerous awards for his technical achievements in these areas. He joined the faculty at the School of Optics and the Center for Research and Education in Optics and Lasers (CREOL) at the University of Central Florida, Orlando, in 1993, and currently holds the positions of Professor of Optics, Electrical and Computer Engineering, and Physics. He has published over 200 articles in referred journals and conference proceedings, has been awarded 12 U.S. patents, and has been recently highlighted on C-SPAN, mainstreekweek.com, and in *Career Encounters*, a PBS Special on technical careers in the optics and photonics field. He is also a Founding Member in the National Science Foundation's Scientists and Engineers in the School Program, which is a program to teach eighth graders about the benefits of science, engineering, and technology in society.

Dr. Delfyett is the Editor-in-Chief of the IEEE JOURNAL OF SELECTED TOPICS IN QUANTUM ELECTRONICS, an Associate Editor of IEEE PHOTONICS TECHNOLOGY LETTERS, was Executive Editor of IEEE LEOS Newsletter (1995–2000), and sits on the Science Advisory Board of the Orlando Science Center and SPIE. He was awarded the 1992 YMCA New Jersey Black Achievement Award, the 1993 National Black Engineer of the Year Award—Most Promising Engineer, the University Distinguished Research Award '99, and was highlighted in *Design News'* "Engineering Achievement Awards". In addition, he has been awarded the National Science Foundation's Presidential Faculty Fellow Early Career Award for Scientists and Engineers, which is awarded to the Nation's top 20 young scientists, the 1999 University Distinguished Researcher of the Year Award, the 2000 Black Engineer of the Year Award—Outstanding Alumnus Achievement, the 2000 Excellence in Graduate Teaching Award, and most recently, the University of Central Florida's 2001 Pegasus Professor Award, which is the highest honor awarded by the University. He also received the Bellcore Synergy Award and the Bellcore Award of Appreciation. He is a Fellow of the Optical Society of America, a Fellow and Board of Governors member of IEEE LEOS, and a member of Tau Beta Pi, Eta Kappa Nu, and Sigma Xi.